

# Characterising the machining of biomedical grade polymers

Barry Aldwell <sup>\*1</sup>, Ray Hanley<sup>2</sup>, and Garret E. O'Donnell<sup>1</sup>

<sup>1</sup>Department of Mechanical and Manufacturing Engineering, Trinity College  
Dublin, Dublin 2, Ireland.

<sup>2</sup>DePuy Ireland, Loughbeg, Ringaskiddy, Co. Cork, Ireland.

**Abstract:** The manufacture of polymer components for biomedical applications is an area which has received much attention from polymer scientists, with high levels of wear resistance achieved, but relatively little research has been done into the machining operations required to manufacture the complex geometries used in total joint replacement. Traditional metal cutting theories have been shown to be insufficient for analysis of polymer machining, as polymers exhibit viscoelastic behaviour, and unique chip formation mechanisms. This paper details an experimental investigation into the effect of tooling and machining parameters on the cutting forces, surface roughness and chip formation in Ultra High Molecular Weight Polyethylene, a common material used in biomedical applications. This research quantifies the relative importance of each parameter, the chip formation mechanisms and resulting surface roughness for the given machining parameters, and provides new insight into applied research on the machining of polymers.

**Keywords:** Polymer, Machining, Sharpness, Chip formation

## 1 Introduction

The machining of polymers is an area which has received relatively little interest from the academic community [1, 2]. While cutting conditions for metals are well understood and well modelled, the viscoelastic behaviour [3] typically seen in polymers complicates analysis and causes some counterintuitive results. Kobayashi [4, 5] was one of the first researchers to perform tests into optimal cutting conditions for a range of polymers.

---

\*Corresponding author. Department of Mechanical and Manufacturing Engineering, Trinity College Dublin, Dublin 2, Ireland. Phone: +353 1 896 1134. Email: aldwellb@tcd.ie

## 1.1 Viscoelastic behaviour of polymers

In viscoelastic materials the strain response to an applied load has both instantaneous, or elastic, and transient, or viscous components. The exact nature of the response is a function of the strain history of the material, the temperature of the material, and the strain rate at which the load is applied [6]. Typically, higher strain rates and lower temperatures will deliver higher moduli. This behaviour can be easily seen in the form of creep under constant applied stress, or stress relaxation under constant applied strain. There is also significant hysteresis associated with load/unload cycles [7, 8].

Above the glass transition temperature the viscous element will dominate the response, while below this temperature the elastic element will dominate [9]. Many polymers have glass transition temperatures below room temperature, so favourable elastic-dominated behaviour can be obtained using low temperature, or cryogenic, machining [10], though this often requires careful consideration of contraction rates [11], and a process control system to maintain the appropriate temperature [12].

## 1.2 Chip formation in polymer machining

Achieving favourable chip formation is one of the main challenges in the machining of polymers [13]. The complex rheological behaviour displayed by polymers means that metal cutting theories are not applicable [14, 15], and that some of the chip formation mechanisms are unique [5]. The types of chip seen in polymer machining are shown in table 1. The continuous chip types are those which are of interest, as discontinuous chips provide poor surface roughness and dimensional accuracy [5]. The continuous - flow\* type of chip<sup>1</sup> is produced by high elastic deformation, and tends to produce chips of similar thickness to the depth of cut, while continuous - shear chips tend to be thicker than the depth of cut, being produced by similar phenomena to that which produces continuous - flow chips in metal cutting. The transition from plastic to elastic yield behaviour complicates analysis, and has implications for cutting forces and temperatures. Chip management after machining is also a challenge, as the chips tend to be ductile, and thus will not break easily, instead wrapping around workpieces and tools, and sometimes interfering with the cutting operation.

## 1.3 Ultra High Molecular Weight Polyethylene

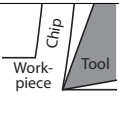
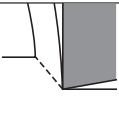
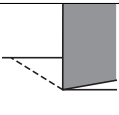
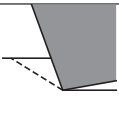
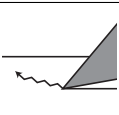
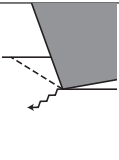
In total joint replacement the use of polymer as a bearing surface in conjunction with metal components is common [16, 17]. In the case of a hip replacement the acetabular cup is manufactured from polymer, while in a knee replacement the condyle surfaces of the tibia are replaced by a polymer insert [18]. Polymers also find use in other areas, such as replacement patellas, and in ankle, shoulder and spinal disc replacement surgery. In these applications the component is subject not only to the standard biomedical rigours of operating in the hostile environment of the human body, but also to mechanical loads, and the inherent issues of creep, fatigue and wear.

UHMWPE (Ultra High Molecular Weight Polyethylene) is an example of a polymer which has found widespread use in the biomedical industry. The popularity of UHMWPE is a result

---

<sup>1</sup>The asterisk is used to denote that this is a different type of chip formation than the similarly named continuous - flow type which is encountered in metal cutting. Flow\* type chips are never formed in metal cutting.

Table 1: Types of chip formed in polymer machining. Shear planes and crack formation are highlighted. Adapted from Kobayashi [5]

Type of chip	Cause	Chip formation
Continuous - Flow*	Produced by high elastic deformation	
Continuous - Shear	Shear plane generated upwards from the point of the cutting tool, shearing occurs along this plane. Continuous because of small shear intervals	
Discontinuous - Simple shear	Shear plane generated upwards from the point of the cutting tool, shearing occurs along this plane. Larger shear intervals, therefore discontinuous chips	
Discontinuous - Complex	Chips are produced by complex stress resulting from the action of a large compressive stress operating in combination with a shear stress	
Discontinuous - Crack	Chip formed by a type of brittle fracture. Cracking around the point of tool	
Discontinuous - Complex (shear with crack)	Crack occurs at a downward angle from the cutting point as well as separation of material along usual shear plane. When the crack grows, a new shear plane forms from the tip of the crack to the free surface and the plastic deformation zone is enlarged	

of the wear characteristics [19] and biocompatibility of the material rather than any inherent machinability or ease of processing [20, 21, 22]. There is little knowledge in the literature about cutting parameters for use with UHMWPE, as manufacturers of biomedical components tend to closely guard their machining parameters [22].

## 1.4 Research aim

This research is being carried out to provide basic insight into the machining of biocompatible polymers above the glass transition temperature. Fundamentally this takes the form of analysis of the effects of machining parameters and tool geometry and sharpness on the cutting forces and chip formation mechanism. Also of interest is the effect of changes in the material, either through additives or through crosslinking of the material, on the machinability of the material. The effect of tool sharpness in particular is not well understood with regards to polymer machining.

## 2 Experimental materials and method

In order to quantify the phenomena occurring during the machining of polymers, a multisensor measurement chain is required [23, 24].

### 2.1 Methodology

The experimental methodology shown in figure 1 was used. It can be seen that this methodology involved an initial phase of material characterisation, subsequent in process measurement of cutting forces and chip formation, and post process measurement to characterise the machined surface and chip. The pre-process measurements were carried out to attempt to measure differences between materials at a molecular level.

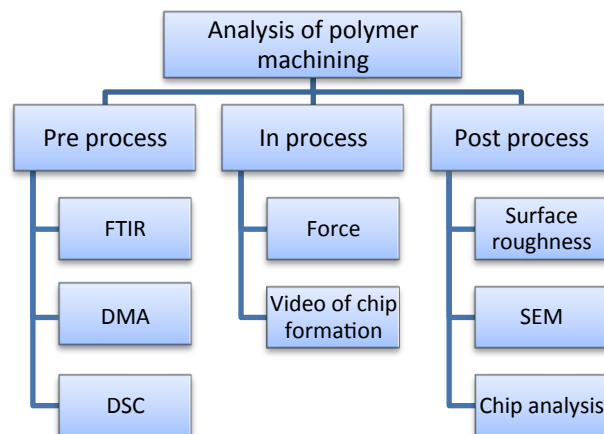


Figure 1: Experimental methodology, showing 3 phases of quantification

### 2.2 Materials under study

Three types of Ultra High Molecular Weight Polyethylene (UHMWPE) were studied:



1. Plain GUR 1020 (UHMWPE)
2. GUR 1020 with antioxidant material added (AOX)
3. Crosslinked GUR 1020 (XLK)

AOX is produced by adding a FDA approved antioxidant material, known as Covernox™, to the base resin before consolidation [25, 26]. The crosslinking process used in the production of XLK was as follows: 50 kGy Gamma irradiation at room temperature, followed by melting at 155°C for 24 hours and annealing at 120°C for 24 hours. Melting and annealing are carried out in a reduced oxygen atmosphere [22].

Typical properties for extruded GUR 1020 are given in table 2. While it is known that crosslinking improves the wear characteristics of UHMWPE, it can also degrade the mechanical properties [27], depending on the process used to crosslink the material. In contrast, the addition of typical antioxidants to UHMWPE has been shown to have little to no effect on static mechanical properties, but may act as a plasticiser [22], which may alter the chip formation mechanism in machining.

Table 2: Properties of extruded GUR 1020. Values are means  $\pm$  standard deviation [22]

Property	Units	Value
Density	$kg/m^3$	$935 \pm 1$
Tensile yield	$MPa$	$22.3 \pm 0.5$
UTS	$MPa$	$53.7 \pm 4.4$
Elongation to failure	%	$452 \pm 19$

### 2.3 Workpiece design

Orthogonal cutting on prepared workpieces was carried out. The workpiece dimensions are shown in figure 2a. The cutting operations were carried out using an Okuma LT15-M, using high speed steel tooling. The constant surface speed feature of the machine was used to provide a constant cutting velocity. The lathe was programmed to carry out machining operations at a range of combinations of cutting speed and depth of cut, with the depth of cut being the feed of the tool into the workpiece disc, in  $mm/revolution$ . The levels used for these parameters are detailed in section 4. It was found that chip buildup lead to issues with corruption of force data. In order to avoid this a slot was cut in the discs, as shown in figure 2b, to prevent a single continuous chip from forming.

### 2.4 Force measurement

Force was measured using a Kistler type 9602 force sensor, mounted as part of a custom toolholder to allow direct force measurement. Calibration was carried out in accordance with ISO 7500-1 [28].

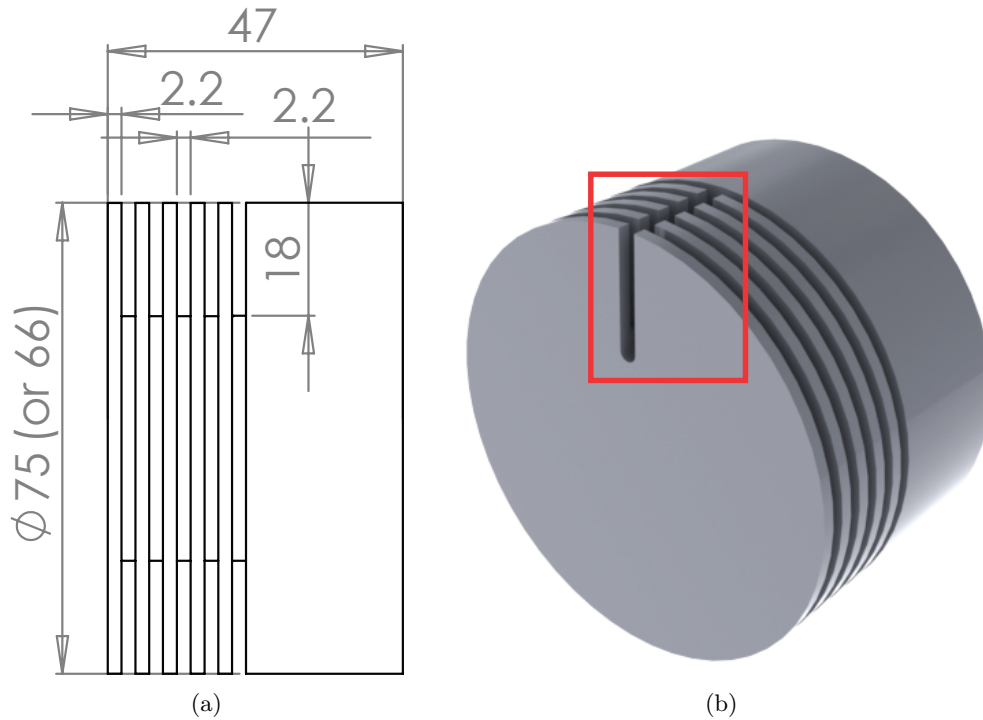


Figure 2: Workpiece design, showing a) Dimensions (mm) and b) Slot cut in discs

## 2.5 Measurement of chip formation

Chip formation was analysed using a high speed camera<sup>2</sup> mounted to the toolholder, with the lens parallel to the axis of the spindle. This allowed a side-on view of the cutting operation. A computer rendering of the mount is shown in figure 3. Chips were also collected from each machining operation, and the cut chip thickness measured five times for each sample.

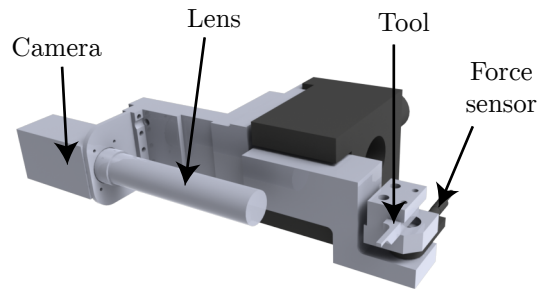


Figure 3: Integration of force and chip formation measurement showing high speed camera mount

## 2.6 Surface roughness measurement

Surface roughness measurement was carried out using a Mitutoyo Surftest SJ-400 portable surface roughness tester. Measurements were carried out on five separate locations on each disc to prevent unusual observations from skewing the results.

<sup>2</sup>A PixelLINK type 782 with Edmund Optics fixed focal length lens, capable of 180 frames per second

## 2.7 Data processing

Data acquisition was carried out using a National Instruments CompactDAQ 9178 carrier, using NI LabVIEW SignalExpress software to record the data. Sample force data is shown in figure 4.

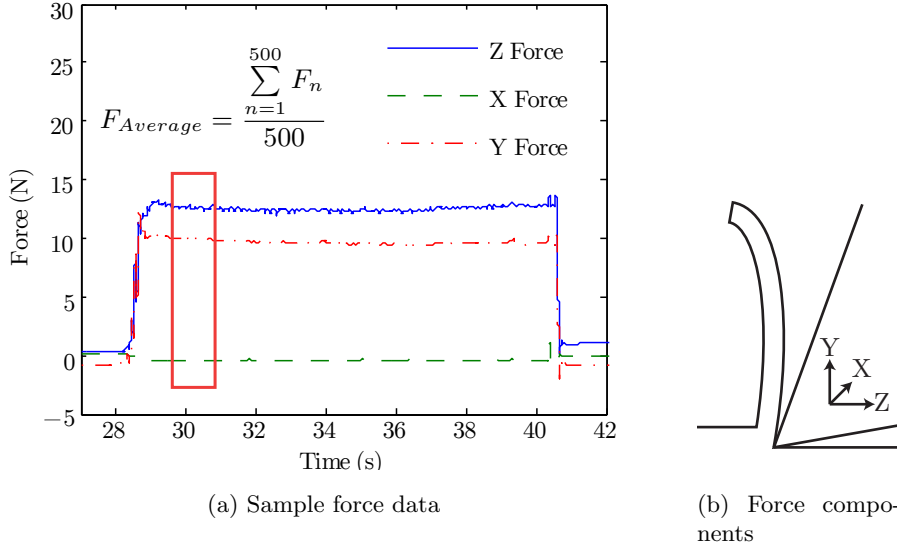


Figure 4: Sample force data, and relationship with cutting forces. Cutting parameters were  $0^\circ$  rake angle, sharp tool,  $155 \text{ m/min}$  cutting speed,  $0.06 \text{ mm/revolution}$  depth of cut, material XLK

From this raw data an average of 500 points of steady state cutting force was extracted for each axis. An average of 500 points was used as in some conditions the duration of the machining operation was  $< 1 \text{ s}$ , and thus it was decided to average over the same number of points, with 500 being found to still allow the extraction of steady state cutting forces for the shorter cuts. The area of interest is highlighted in figure 4. It can be seen from figure 4b that the Z force corresponds to the cutting force, while the Y force corresponds to the thrust force. In order to compensate for any errors in the mounting of the force sensor, the resultant of the X and Y forces was used as the thrust force. Statistical analysis was performed on this extracted data using Minitab 16.

## 3 Analysis of tool-workpiece engagement

The effect of increasing edge radius can be expressed by the ratio of the edge radius  $r$  and the depth of cut, as defined in equation 1.

$$\frac{r}{DOC_{Nominal}} \quad (1)$$

The effect of this parameter on cutting is shown in figure 5. In the case of a tool with negligible tool radius and a correspondingly small ratio, as shown in figure 5a, there will be a single well defined cutting point, minimal contact on the rake face, and close to zero contact on the clearance face of the tool. Increasing the edge radius, as shown in figure 5b, increases the contact areas on these two faces, thus increasing friction. This increase in friction will generate more heat and

increase cutting forces, and the increased contact area on both faces of the tool will allow a larger heat flux to be transmitted to the tool. This is taken to an extreme level in figure 5c, where the edge radius exceeds the depth of cut, and the material is compressed rather than cut by the tool. In this case any material removal is likely to be due to compressive cracking of the material, leading to spalling of a layer of material after the tool has passed, and an extremely rough cut surface. There may also be a reduction in heat transmission to the tool, due to the lack of a chip in contact with the rake face of the tool.

In a viscoelastic material such as UHMWPE it is anticipated that workpiece deformation will occur [4], even in favourable cutting conditions. If the cutting forces have a large component into the workpiece then the material will have been compressed, and will tend to return to an undeformed state after the tool has passed. As discussed previously, polymers have viscoelastic responses to applied loads, so any expansion of the material after removal of a compressive force will have elastic and viscous components. The elastic component is shown in figure 5, where it manifests as a difference between the nominal depth of cut, which is the displacement or penetration of the tool below the original surface of the material, and the instantaneous depth of cut, which will be less than the nominal value due to the material expanding after unloading. Expansion of the material due to viscous relaxation over time will also alter the effective depth of cut. Thus the depth of cut has three components: the nominal depth of cut, the instantaneous expansion after unloading, and expansion over time due to viscoelastic relaxation.

It is worthy of note that as the ratio of edge radius to depth of cut increases the cut surface experiences what is effectively a negative rake angle. When the edge radius approaches or exceeds the depth of cut, as shown in figure 5c, the nominal rake angle of the tool is no longer a factor, as only the rounded edge is in contact with the workpiece.

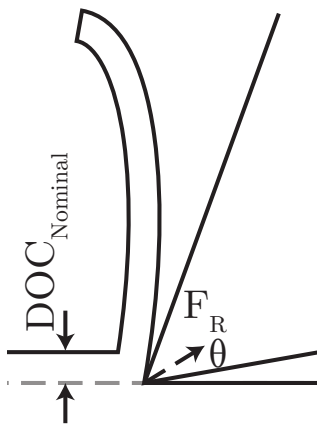
## 4 Design of experiments

In order to identify dominant factors a full factorial experiment was undertaken. The factors and levels used are shown in table 3. All tests were performed without the use of coolant, with each test being performed once. The factors were chosen to allow analysis of the effect of material and tool geometry and sharpness, while also reflecting the effect of machining parameters.

Table 3: Factors used in design of experiments

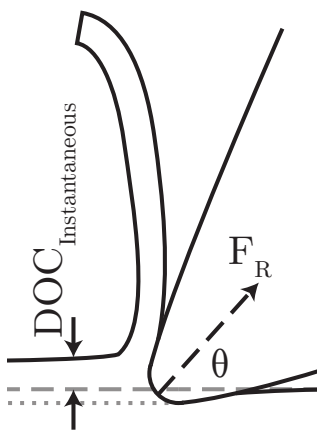
Factor	Number of levels	Levels
Material	3	See section 2.2
Rake angle	4	$-20^\circ$ , $0^\circ$ , $20^\circ$ , $40^\circ$
Edge radius	3	Sharp, worn, highly worn - See table 4
Cutting speed	2	155, 300 <i>m/min</i>
Depth of cut	2	0.06, 0.19 <i>mm/rev</i>

The levels for material correspond to the materials under study, while the rake angles were chosen to allow comparison with the work of Kobayashi [5], and to reflect a range of rake angles typically used in industry. The edge radii corresponding to each sharpness are shown in table



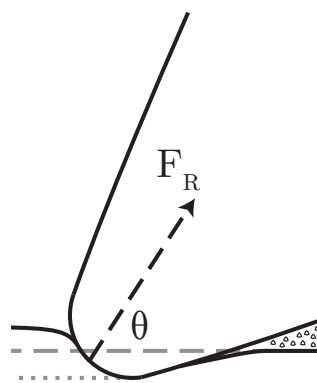
- $\frac{r}{DOC} \approx 0$
- Little workpiece deformation
- No difference between nominal and actual depth of cut
- Continuous chip
- Low cutting forces
- Small contact area

(a) Sharp tool



- $\frac{r}{DOC} < 1$
- Some workpiece deformation
- Some difference between nominal and actual depth of cut
- Continuous chip
- Higher cutting forces
- Increased contact area

(b) Worn tool



- $\frac{r}{DOC} > 1$
- Large workpiece deformation
- Large difference between nominal and actual depth of cut
- Discontinuous chip – potentially spalling
- High contact forces
- Large contact area on clearance face – little contact on rake face

(c) Highly worn tool

Figure 5: Cutting arrangement for increasing tool edge radius  $r$ . Adapted from [29, 30]

4, along with the maximum values of the ratio between edge radius and depth of cut for each sharpness level. The sharpness levels were based upon observations from industrial investigations, and depth of cut levels were then chosen to provide a range of values for the ratio between edge radius and depth of cut from close to zero to greater than one. The cutting speed levels were chosen to provide a large range within the capabilities of the machine used, while allowing comparison with past work.

Table 4: Sharpness levels

Level	Edge radius ( $\mu m$ )	Maximum $\frac{r}{DOC}$
Sharp	10–15	0.25
Worn	40–60	1
Highly worn	80–120	2

The following responses were used for statistical analysis:

1. Cutting force,  $F_c$
2. Thrust force,  $F_t$
3. Surface roughness,  $R_a$
4. Cut chip thickness

In addition, visual data from the high speed camera and SEM were examined on a qualitative basis.

## 5 Results and discussion

### 5.1 Analysis of variance methodology

As mentioned in section 2.7, statistical analysis was performed using Minitab 16. This took the form of a General Linear Model for each response. Details of the ANOVA conditions can be found in table 5.

Table 5: ANOVA conditions for each response

Response	Interactions studied	$R^2$	Significance level
$F_c$	4 way	99.48	0.05
$F_t$	4 way	99.73	0.05
$R_a$	5 way	81.65	0.05
Chip thickness	3 way	99.78	0.05

## 5.2 Cutting force

The main effects for cutting force are shown in figure 6. Cutting force increases with depth of cut and tool wear, as expected, and decreases with rake angle, indicating easier cutting at higher rake angles. Workpiece material has a small effect, with plain UHMWPE showing higher forces than AOX or XLK. This may indicate that the addition of antioxidant or the crosslinking of the material has an adverse effect on the mechanical properties of the material, with the antioxidant effect due to the additive acting as a plasticiser. It is possible that the relatively small effect of cutting speed is a result of the effects of increased strain rate and softening of material due to frictional heating offsetting each other at the levels used.

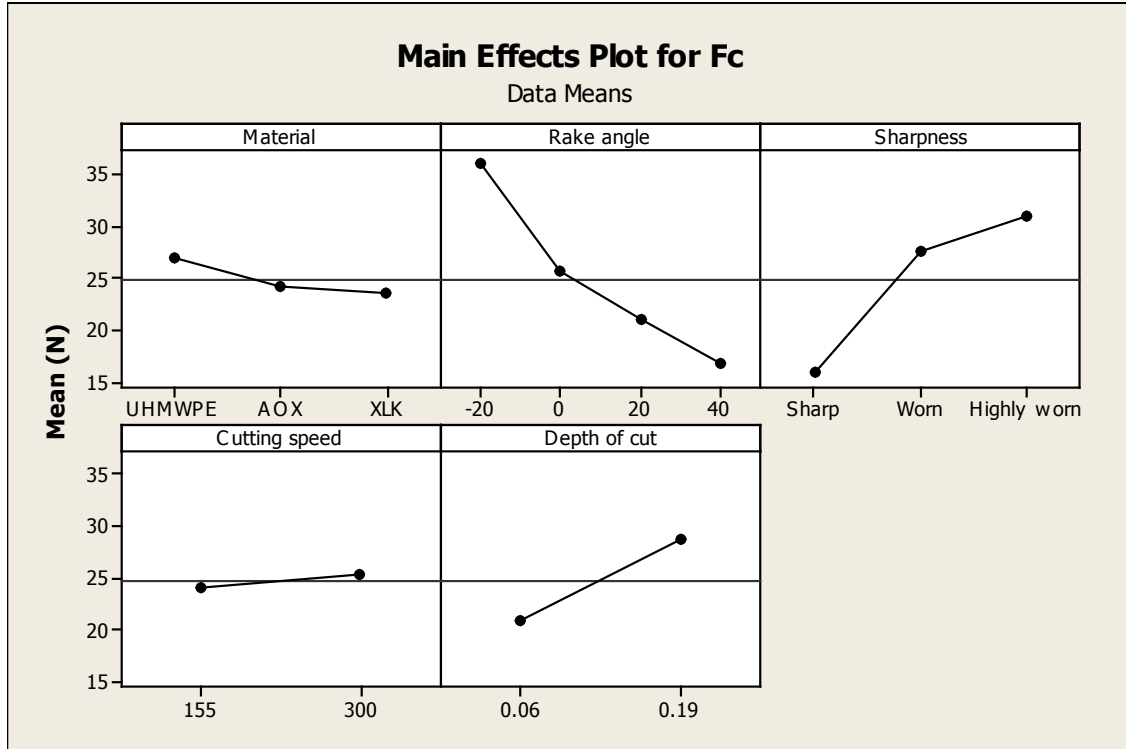


Figure 6: Main effects plot for cutting force

The two way interactions for cutting force are shown in figure 7, with a full table of P values from the ANOVA shown in A. 6 of the 10 two way interactions appear significant, with the material - depth of cut interaction being marginally significant ( $P = 0.045$ ). The interactions of rake angle with sharpness, depth of cut and material may indicate a change in chip formation mechanism, and the influence of the size effect on the transition from cutting to material deformation at low rake angle and/or large edge radius, as discussed in section 3.

In addition, the three way interactions of material - rake angle - sharpness and rake angle - sharpness - depth of cut were significant, as was the four way interaction of rake angle - sharpness - cutting speed - depth of cut. This complex dependency of cutting force on the cutting parameters further indicates that transitions in chip formation mechanism are occurring within the parameter levels studied. Of interest is that cutting speed has the highest P value of the main effects and

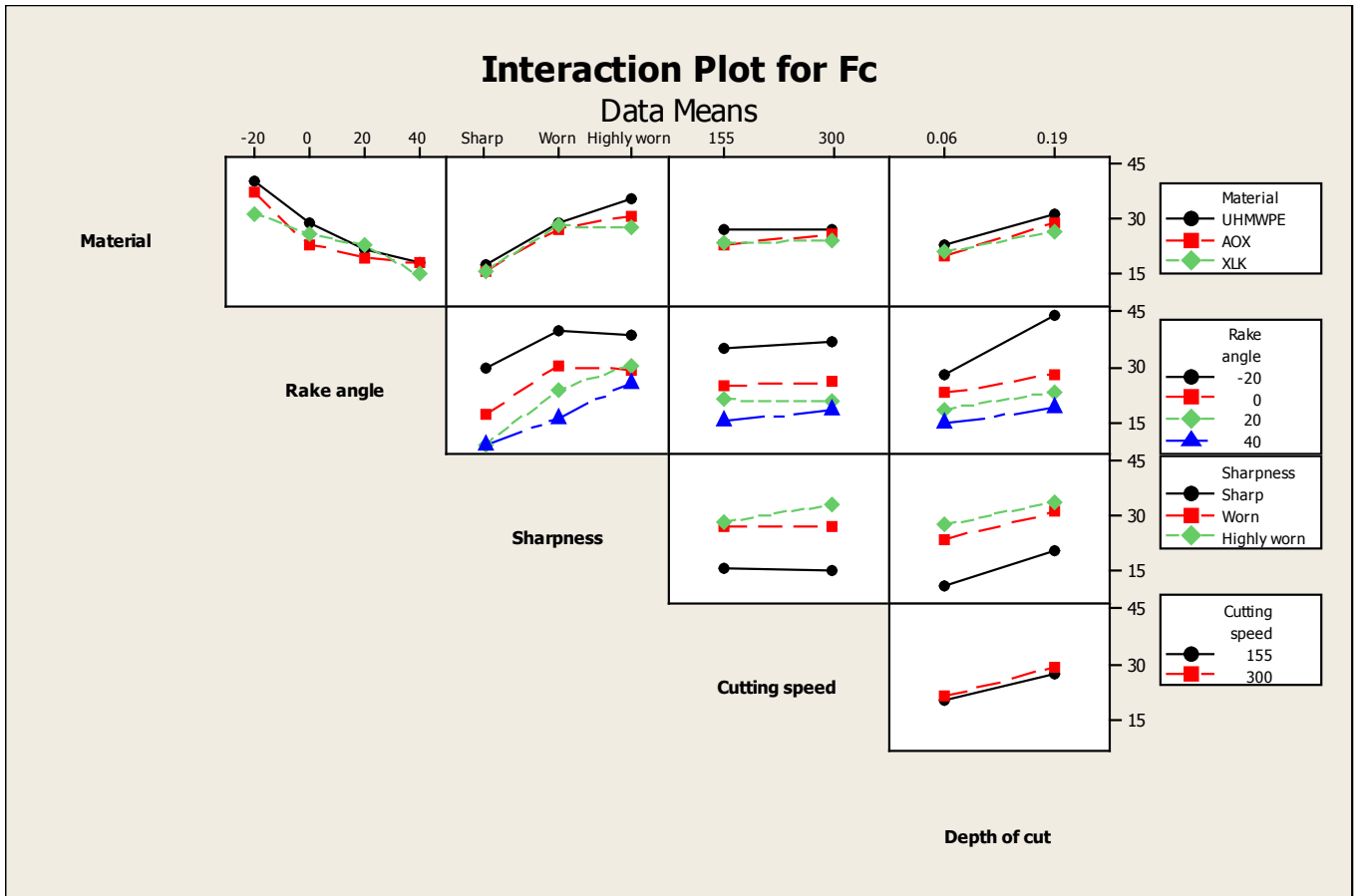


Figure 7: Interaction plot for cutting force

is significant in only a single two way interaction and no three way interactions, but is significant in the four way interaction. This indicates a relatively weak overall effect from cutting speed compared to the other factors.

### 5.3 Thrust force

The main effects for thrust force are shown in figure 8. The same overall trends hold as for cutting force, with the exception of depth of cut, with thrust force decreasing with increasing depth of cut. This is consistent with the analysis shown in section 3, as for the large depth of cut the ratio of edge radius to depth of cut remained small for all cutting operations.

The two way interactions for cutting force are shown in figure 9, with a full table of P values from the ANOVA shown in A. 7 of the 10 two way interactions appear significant, with the material - cutting speed interaction being marginally significant ( $P = 0.048$ ), as the material - depth of cut interaction was for cutting force. Compared to the two way interactions for cutting force the interaction between sharpness and depth of cut is now highly significant, indicating the effect of the ratio of edge radius and depth of cut, as defined in equation 1. This ratio remains small for large depths of cut, but exceeds 1 for small depths of cut, leading to increased thrust force, and thus the interaction between sharpness and depth of cut.



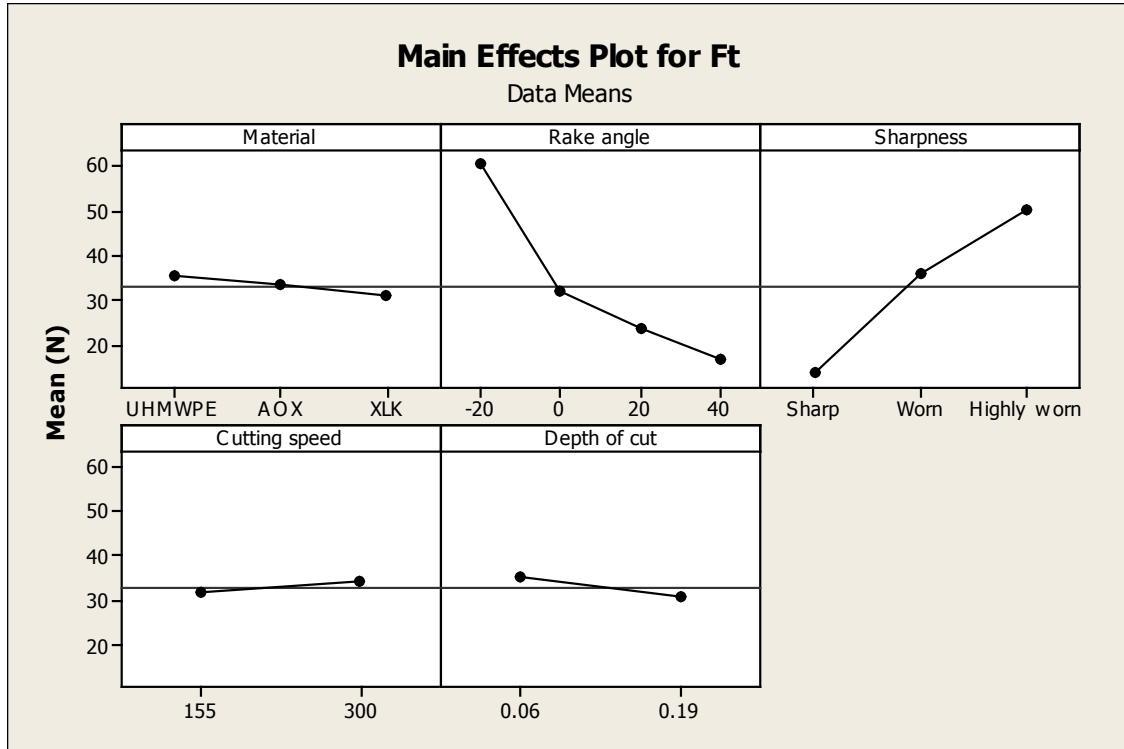


Figure 8: Main effects plot for thrust force

The three and four way interactions for thrust force show the same pattern as for cutting force. The high  $R^2$  values for cutting force and thrust force (99.48 and 99.73, respectively) show that the model contains little unexplained variation, and thus can be considered accurate for analysis purposes.

## 5.4 Surface roughness

The main effects for surface roughness are shown in figure 10. Due to the extremely rough nature of the machined surfaces for highly worn tools, as shown in section 5.6.1, it was decided to restrict analysis to sharp and worn tools. It is clear that the change in sharpness from sharp to worn has a large effect on surface roughness. A higher depth of cut gives a better surface roughness. The main effects plot for material shows AOX giving a higher surface roughness result on average compared to UHMWPE and XLK, which could suggest a slight change in chip formation mechanism in AOX compared to UHMWPE and XLK, again possibly due to the additive acting as a plasticiser.

The two way interactions for surface roughness are shown in figure 11. The ANOVA indicates that all of the two way interactions are significant, with the exception of the cutting speed - depth of cut interaction. There is an interaction between sharpness and depth of cut due to the size effect, as the maximum  $\frac{r}{DOC}$  for worn tools was 1, which would cause poor cutting at low depths of cut with worn tools, thus giving poor surface finish. In addition, rake angle appears to be exhibiting complex behaviour, with a strong interaction between rake angle and sharpness. For

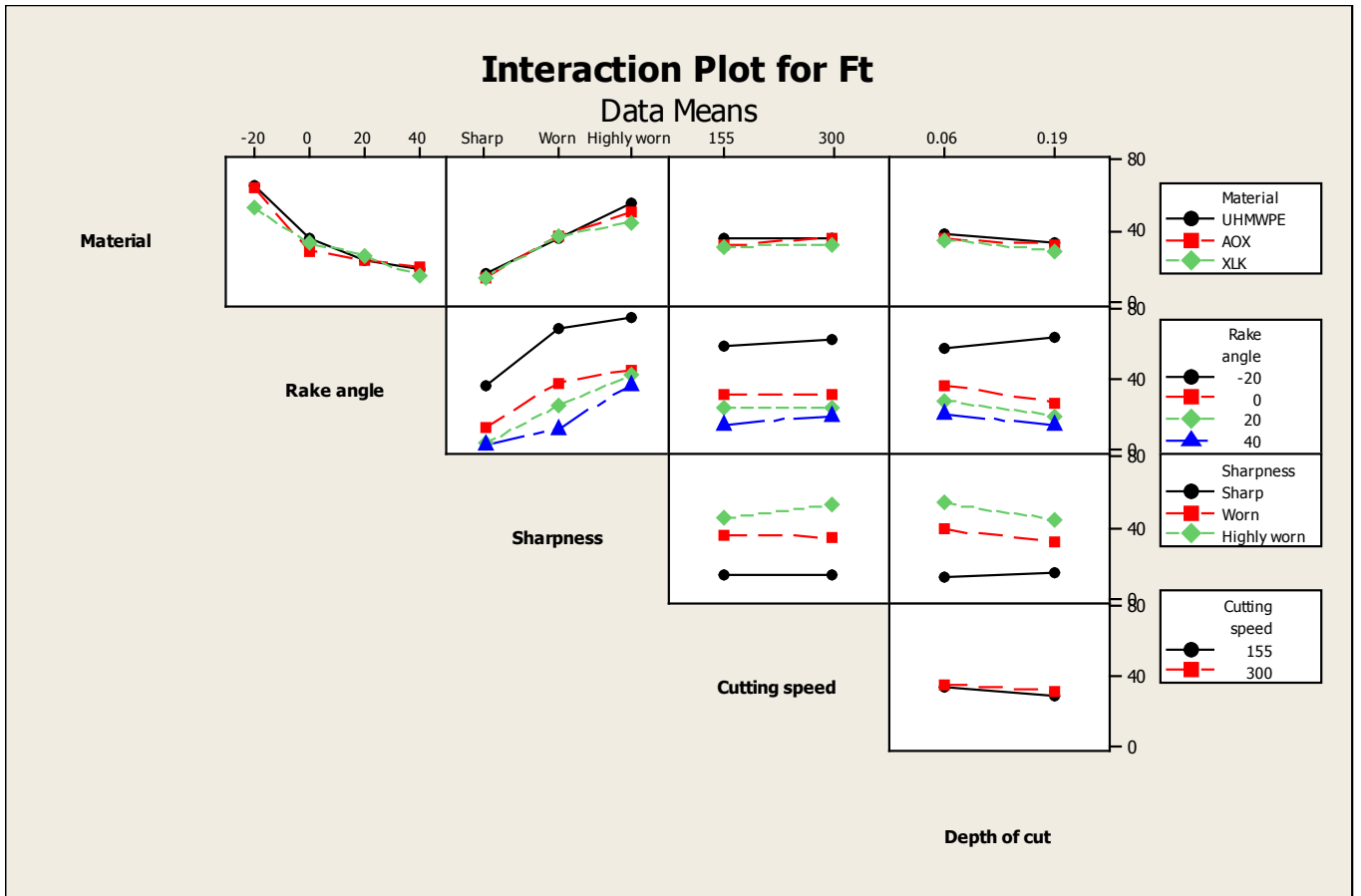


Figure 9: Interaction plot for thrust force

both sharp and worn tools the result at a rake angle of  $20^\circ$  is greater than that of  $0^\circ$  and  $40^\circ$ . Similar increases at rake angles between  $5^\circ$  and  $10^\circ$  have been reported in the past [31]. This could be an effect associated with the critical rake angle, as for the cutting conditions used the critical rake angle would be in the region of  $5^\circ$  to  $20^\circ$ , as discussed by Kobayashi [5].

The ANOVA also indicates that all but one of the three way interactions, all of the four way interactions, and the five way interaction are all significant. This, coupled with the  $R^2$  value of 81.65 and a lack of normal residuals (Anderson - Darling test P value  $< 0.005$ ) leads to the conclusion that there is variation which is unexplained by this model, which requires further investigation.

## 5.5 Chip thickness

The main effects for the difference between cut and uncut chip thicknesses are shown in figure 12. Worn and highly worn tools did not produce a continuous chip in all machining conditions, so this analysis was only performed on data from experiments performed with sharp tools. The low correlation between depth of cut and chip thickness is expected, as the variation due to depth of cut has been removed. It is clear that the  $-20^\circ$  rake angle produces, on average, a chip which is significantly thicker than the uncut chip thickness, indicating that negative rake angle cutting is



Figure 10: Main effects plot for surface roughness

of the continuous - shear type, as detailed in table 1. Cutting at neutral and positive rake angles produces a difference close to zero, indicating that the cut is of the continuous - flow\* type. The ANOVA indicates that cutting speed is not statistically significant for chip thickness ( $P = 0.172$ ).

The two way interactions for chip thickness are shown in figure 13. The interactions involving cutting speed are all statistically insignificant ( $P > 0.131$  in all cases), while all other two way interactions are significant ( $P < 0.021$  in all cases), with the rake angle - depth of cut interaction having the most striking effect. It is clear from the interactions that the behaviour at the negative rake angle gives much higher chip thickness than at neutral or positive rake angles. The plain UHMWPE and crosslinked material have similar behaviour, while the material with added antioxidant has a consistently lower chip thickness at all rake angles, indicating that the addition of antioxidant changes the chip formation mechanism slightly, as suggested by the surface roughness result, giving further evidence to the plasticiser hypothesis.

Only one three way interaction is significant for chip thickness, the material - cutting speed - depth of cut interaction, possibly indicating that the plasticising effect of the additive is sensitive to machining conditions. This is the only level at which cutting speed appears significant for chip thickness, indicating an extremely weak effect overall.

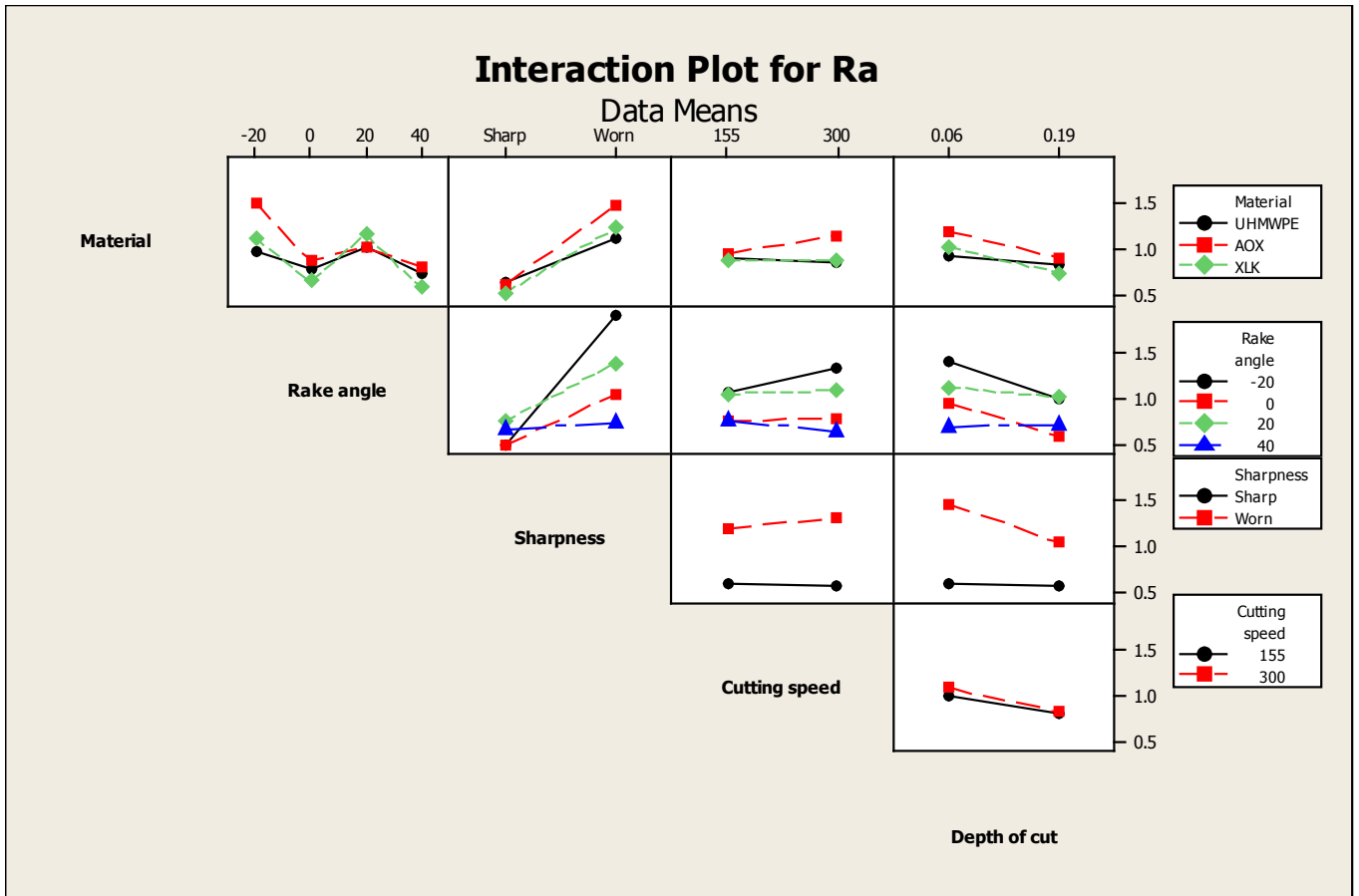


Figure 11: Interaction plot for surface roughness

## 5.6 SEM and high speed video

### 5.6.1 Varying sharpness

The effect of varying tool sharpness on the surface finish is shown in figure 14, with high speed video of chip formation at low depths of cut shown in figure 15. An example of favourable cutting conditions is shown in figure 15a. There is a single cutting edge evident, with no contact on the clearance face and little contact between the chip and the rake face. A smooth continuous chip of the same thickness as the depth of cut is being formed. The machined surface is shown in figure 14a. Based upon chip thickness results it appears that the continuous - flow\* chip formation mechanism is occurring when the sharp tool is used.

It is clear that while there is a slight degradation in surface quality when the tool is worn, transition to the highly worn state causes a marked decrease in the quality of the machined surface. The chip formation for a worn tool, shown in figure 15b, shows some workpiece deformation around the cutting edge, and contact between the workpiece and the clearance face of the tool, but there is still a continuous chip being formed, indicating that the continuous - flow\* chip formation mechanism is still occurring.

The surface shown in figure 14c displays an undulating machined surface, unlikely to be of use in any engineering application. The chip formation for this cutting condition is shown in figure

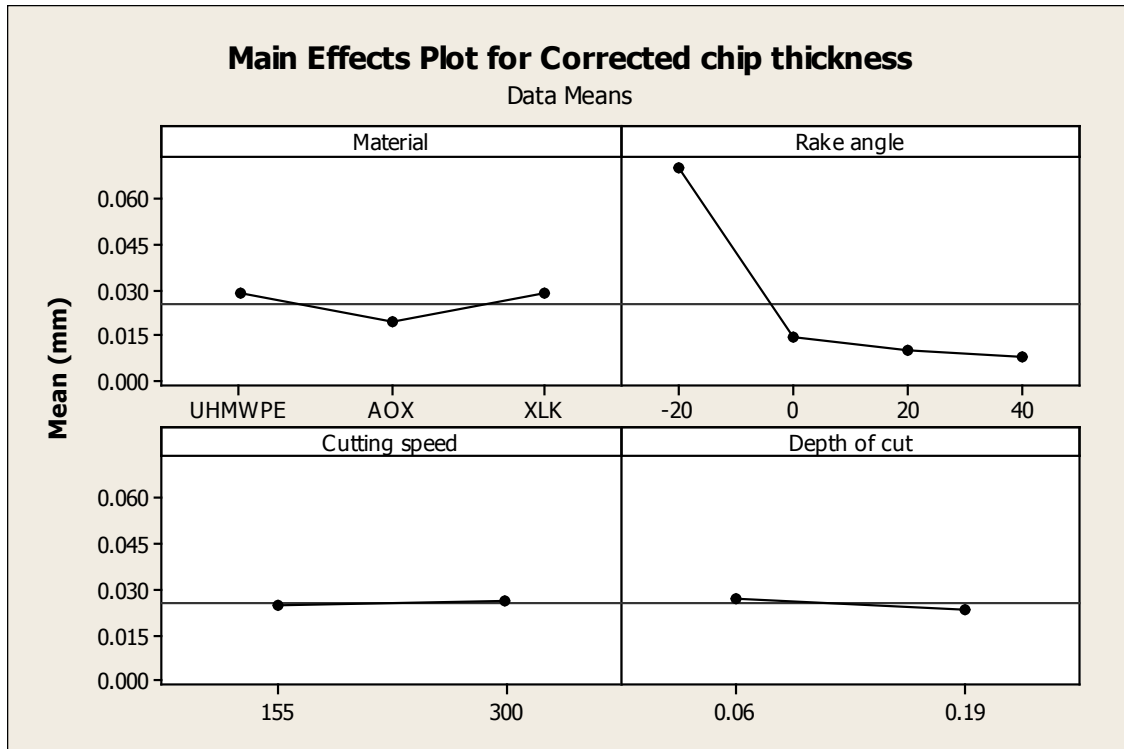


Figure 12: Main effects plot for chip thickness

15c. There is a discontinuous chip of either the discontinuous - simple shear or the discontinuous - crack type being formed, with very large deformation of the workpiece occurring before the cutting point of the tool, and contact between the workpiece and the clearance face of the tool. This is an example of machining with a tool edge radius exceeding the depth of cut, as detailed in section 3. The expansion of the workpiece after the tool has passed is also evident, as discussed in section 3.

### 5.6.2 Varying rake angle

The effect of varying tool rake angle on the surface finish is shown in figure 16, with high speed video of chip formation at low depths of cut shown in figure 17. For all 4 rake angles studied the SEM images for sharp tools show a surface which appears free of major defects, and reflects the profile of the tool used in machining. There is nothing to disagree with the surface roughness results for sharp tools given in section 5.4.

High speed images show continuous chip formation for all rake angles, with some workpiece deformation evident at the negative rake angle, as shown in figure 17a. The chip formation mechanism at the negative rake angle appears to be continuous - shear, while at the neutral and positive rake angles it appears to be continuous - flow\*.

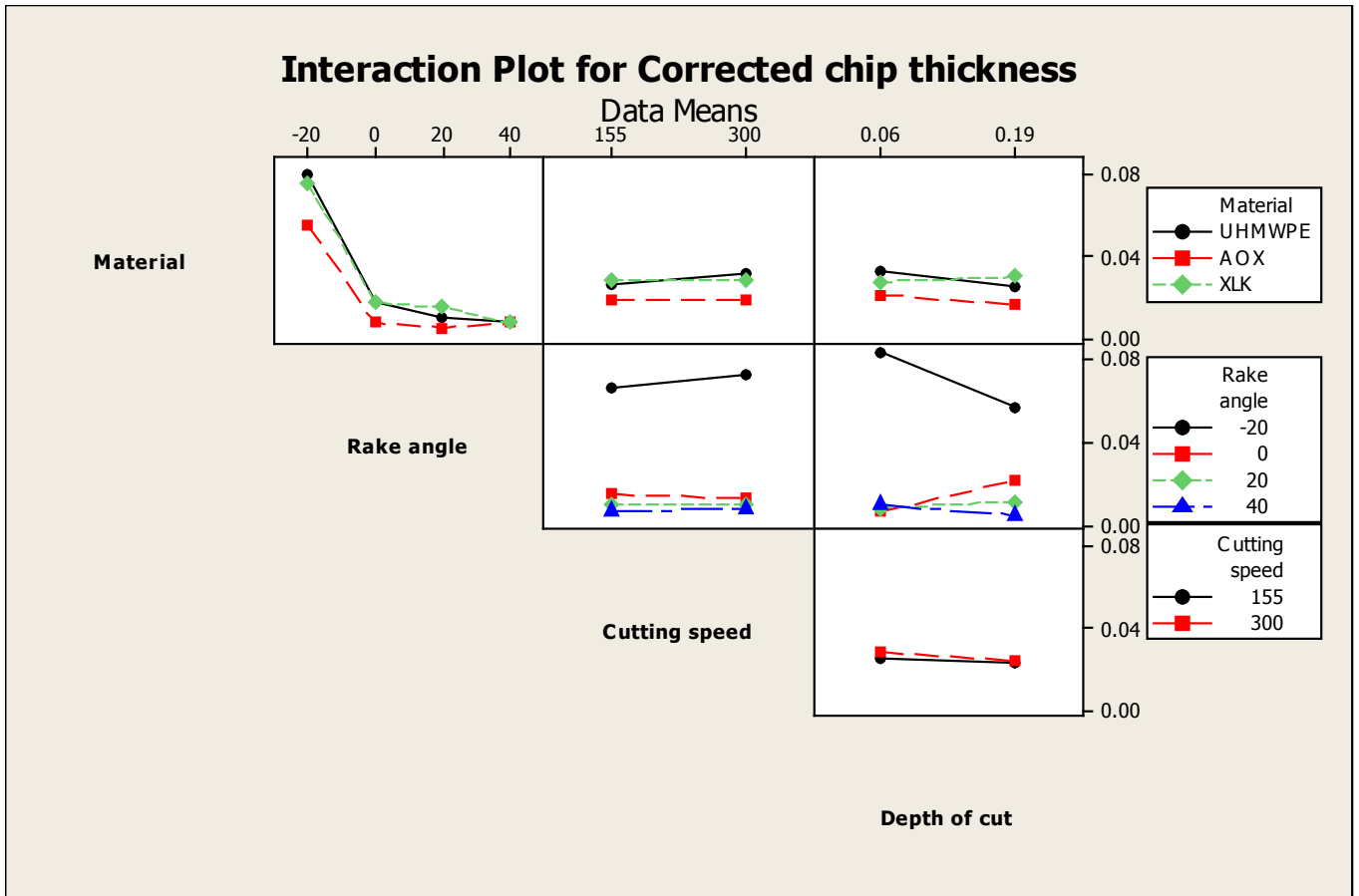


Figure 13: Interaction plot for chip thickness

## 6 Conclusion

A preliminary investigation into the effect of tool sharpness, rake angle and machining parameters on the machining of UHMWPE was carried out, and statistical analysis performed on the results. From this the following conclusions can be drawn:

- At low depths of cut with worn tools the area of engagement between the tool and workpiece will present what is effectively a negative rake angle to the workpiece. Negative rake angles deliver higher forces, temperature, surface roughness and chip thickness than neutral or positive rake angles. The chip thickness result for negative rake angle tools indicates that chip formation is of the continuous - shear type, while the continuous - flow\* chip formation mechanism is occurring at positive rake angles. This change in chip formation mechanism may account for the increased forces, temperature and surface roughness, as the material is undergoing different yield behaviour.
- The models for cutting force, thrust force and chip thickness displayed high  $R^2$  values, indicating that almost all of the variation in the responses was explained by the factors used in the analysis. Conversely, the model for surface roughness had a  $R^2$  value of 81.65, indicating that there is unexplained variation in this response. Further investigation is required to

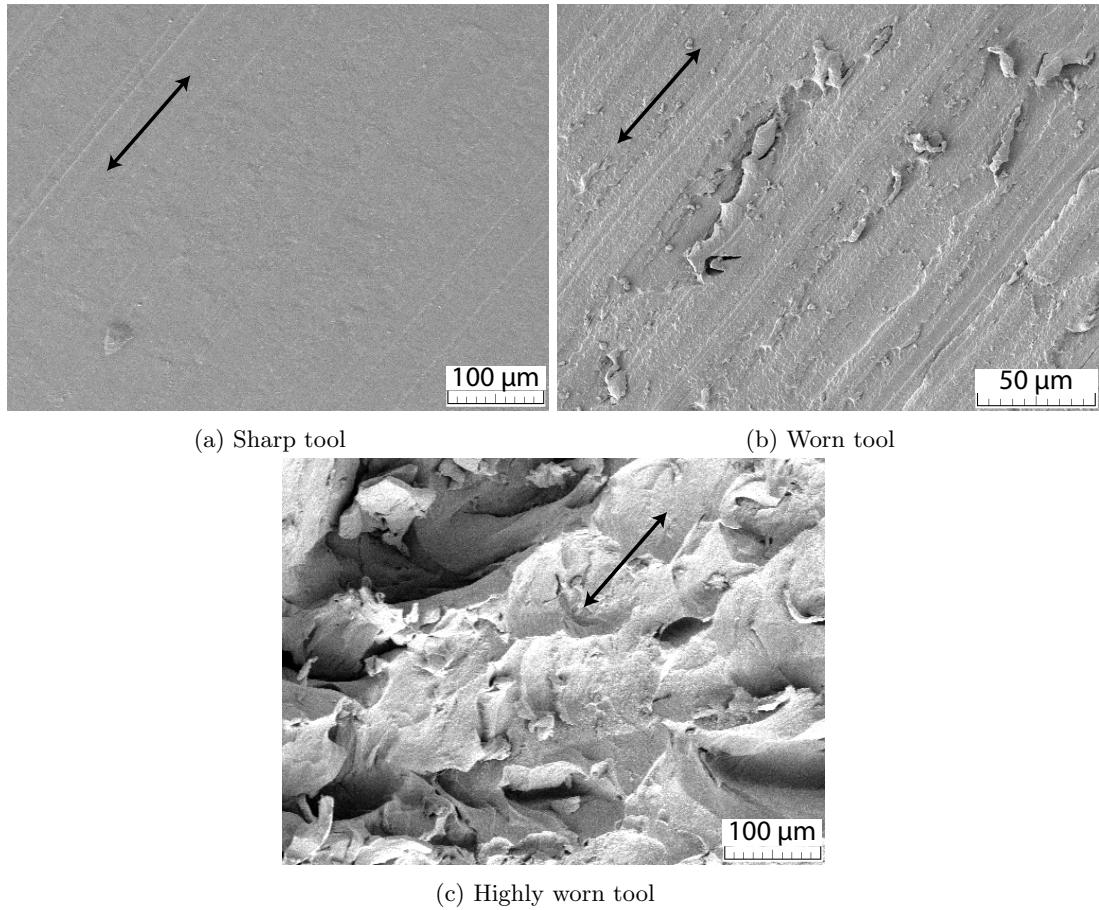


Figure 14: SEM images showing effect of varying tool sharpness. Arrows show direction of cut. Material is XLK, rake angle is  $40^\circ$ , cutting speed  $155\text{ m/min}$  and depth of cut  $0.06\text{ mm}$

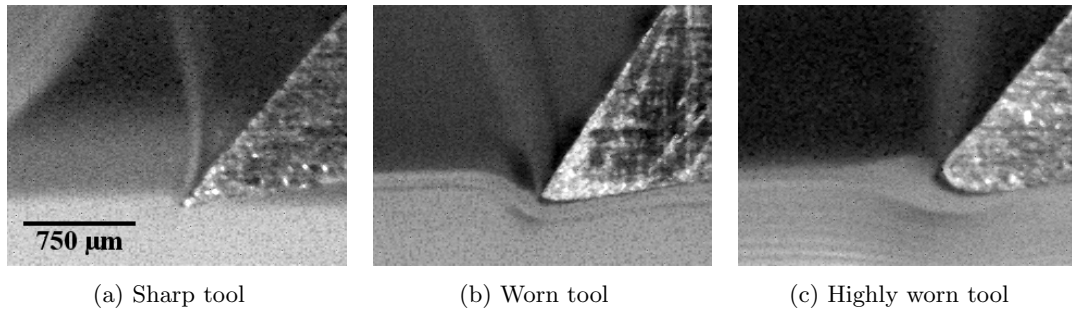


Figure 15: High speed camera images showing effect of varying tool sharpness at low depth of cut. Workpiece moving left to right relative to tool

evaluate the source of this unexplained variation, either with a non-linear statistical model, or through including variables not included in the model presented in this paper, such as the variations in the profile of each individual tool cutting edge due to the grinding and sanding required to achieve the required surface roughness.

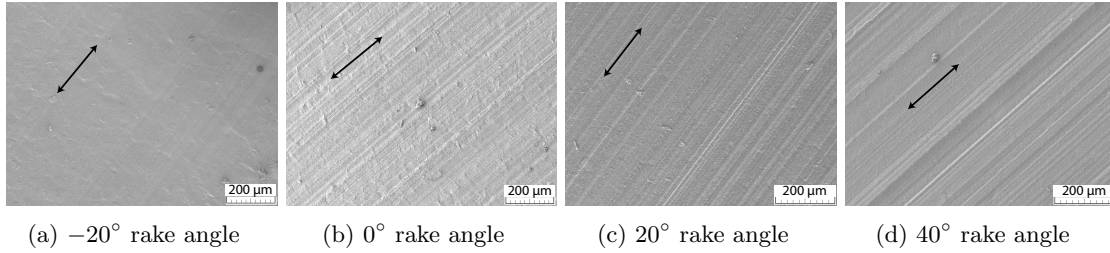


Figure 16: SEM images showing effect of varying tool rake angle for sharp tools. Arrows show direction of cut

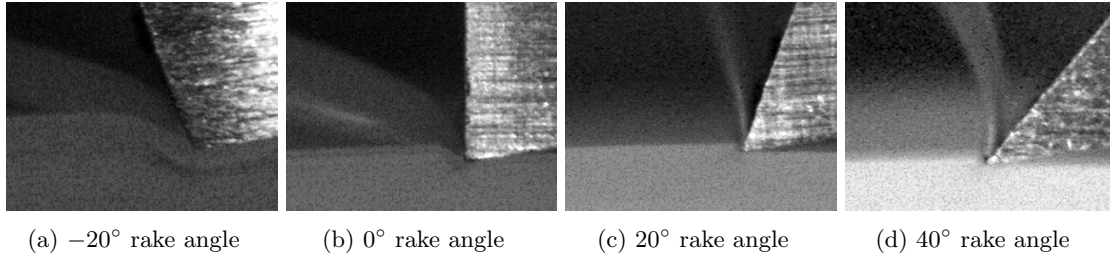


Figure 17: High speed camera images showing effect of varying tool rake angle at low depth of cut. Workpiece moving left to right relative to tool

- Cutting speed was found to be the least significant factor out of the five responses measured. This leads to a hypothesis that the stiffening effect of a higher strain rate and the softening effect of higher frictional heating may offset each other, within the parameters used. Further investigation is warranted to ascertain the exact effect of cutting speed.
- There exists a large two way interaction between tool rake angle and edge radius for the response of workpiece surface roughness. This can be important for tool life analyses, as a larger rake angle will deliver acceptable surface roughness for longer. Conversely, using a negative rake angle and/or allowing the tool to blunt excessively will lead to extremely poor surface finish.
- Workpiece deformation around the cutting edge increases dramatically as edge radius increases. This is reflected in an increase in force on the tool, particularly the thrust force. This indicates that the tool is compressing the workpiece as it cuts, which for a viscoelastic material such as polyethylene may lead to issues with workpiece relaxation, which will cause problems with dimensional accuracy in a manufacturing environment. Further work is required to effectively characterise the effect of compressive cutting forces on polymer relaxation.

## Acknowledgements

Thanks must be given to J.J. Ryan of the Department of Mechanical and Manufacturing Engineering, Trinity College Dublin, for his assistance during testing.



## Funding

The authors gratefully acknowledge the support of DePuy Ireland and the Irish Research Council for this ongoing research project.

## References

- [1] Dhokia V, Kumar S, Vichare P, Newman S, Allen R. Surface roughness prediction model for CNC machining of polypropylene. *Proceedings of the Institution of Mechanical Engineers, Part B: Journal of Engineering Manufacture*. 2008;222(2):137 – 157.
- [2] Dhokia VG, Kumar S, Vichare P, Newman ST. An intelligent approach for the prediction of surface roughness in ball-end machining of polypropylene. *Robotics and Computer-Integrated Manufacturing*. 2008;24(6):835 – 842.
- [3] Xiao KQ, Zhang LC. The role of viscous deformation in the machining of polymers. *International Journal of Mechanical Sciences*. 2002;44(11):2317 – 2336.
- [4] Kobayashi A, Saito K. On the cutting mechanism of high polymers. *Journal of Polymer Science*. 1962;58(166):1377 – 1396.
- [5] Kobayashi A. *Machining of plastics*. McGraw-Hill; 1967.
- [6] Kurtz SM, Villarraga ML, Herr MP, Bergström JS, Rinnac CM, Edidin AA. Thermomechanical behavior of virgin and highly crosslinked ultra-high molecular weight polyethylene used in total joint replacements. *Biomaterials*. 2002;23(17):3681 – 3697.
- [7] Krzypow DJ, Rinnac CM. Cyclic steady state stress – strain behavior of UHMW polyethylene. *Biomaterials*. 2000;21(20):2081 – 2087.
- [8] Avanzini A. Effect of cyclic strain on the mechanical behavior of virgin ultra-high molecular weight polyethylene. *Journal of the Mechanical Behavior of Biomedical Materials*. 2011;4(7):1242 – 1256.
- [9] Kakinuma Y, Kidani S, Aoyama T. Ultra-precision cryogenic machining of viscoelastic polymers. *CIRP Annals - Manufacturing Technology*. 2012;61(1):79 – 82.
- [10] Ervine P, O'Donnell GE. An overview of the machining of polymer materials. In: *Proceedings of the 26th International Manufacturing Conference, 2nd-4th September 2009*; 2009. p. 145 – 153.
- [11] Dhokia VG, Newman ST, Crabtree P, Ansell MP. A methodology for the determination of foamed polymer contraction rates as a result of cryogenic CNC machining. *Robotics and Computer-Integrated Manufacturing*. 2010;26(6):665 – 670.
- [12] Dhokia VG, Newman ST, Crabtree P, Ansell MP. A process control system for cryogenic CNC elastomer machining. *Robotics and Computer-Integrated Manufacturing*. 2011;27(4):779 – 784.
- [13] Shokrani A, Dhokia V, Newman ST. Environmentally conscious machining of difficult-to-machine materials with regard to cutting fluids. *International Journal of Machine Tools and Manufacture*. 2012;57(0):83 – 101.
- [14] Wyeth DJ. An investigation into the mechanics of cutting using data from orthogonally cutting Nylon 66. *International Journal of Machine Tools and Manufacture*. 2008;48(7 - 8):896 – 904.

- [15] Wyeth DJ, Atkins AG. Mixed mode fracture toughness as a separation parameter when cutting polymers. *Engineering Fracture Mechanics*. 2009;76(18):2690 – 2697.
- [16] Kutz M. *Handbook of materials selection*. Wiley Online Library; 2002.
- [17] Sobieraj MC, Rinnac CM. Ultra high molecular weight polyethylene: Mechanics, morphology, and clinical behavior. *Journal of the Mechanical Behavior of Biomedical Materials*. 2009;2(5):433 – 443.
- [18] Kurtz SM, Muratoglu OK, Evans M, Edidin AA. Advances in the processing, sterilization, and crosslinking of ultra-high molecular weight polyethylene for total joint arthroplasty. *Biomaterials*. 1999;20(18):1659 – 1688.
- [19] Turell ME, Friedlaender GE, Wang A, Thornhill TS, Bellare A. The effect of counterface roughness on the wear of UHMWPE for rectangular wear paths. *Wear*. 2005;259:984 – 991.
- [20] Oral E, Neils AL, Lyons C, Fung M, Doshi B, Muratoglu OK. Surface cross-linked UHMWPE can enable the use of larger femoral heads in total joints. *Journal of Orthopaedic Research*. 2012;31:59 – 66.
- [21] Oral E, Christensen SD, Malhi AS, Wannomae KK, Muratoglu OK. Wear resistance and mechanical properties of highly cross-linked, ultrahigh-molecular weight polyethylene doped with vitamin E. *The Journal of arthroplasty*. 2006;21(4):580 – 591.
- [22] Kurtz SM. *UHMWPE Biomaterials Handbook, Second Edition: Ultra High Molecular Weight Polyethylene in Total Joint Replacement and Medical Devices*. Elsevier; 2009.
- [23] Teti R, Jemielniak K, O'Donnell GE, Dornfeld D. Advanced monitoring of machining operations. *CIRP Annals - Manufacturing Technology*. 2010;59(2):717 – 739.
- [24] Aldwell B, Hanley R, O'Donnell GE. The Development of a Measurement Chain for the Monitoring and Analysis of Polymer Machining. In: *The Proceedings of the 29th International Manufacturing Conference*; 2012. .
- [25] Brockett C, Hardaker C, Fisher J, Jennings L. The Wear of a New Total Knee Replacement With Anti-Oxidant UHMWPE. *Bone & Joint Journal Orthopaedic Proceedings Supplement*. 2013;95-B(SUPP 15):139.
- [26] Oral E, Neils AL, Rowell SL, Lozynsky AJ, Muratoglu OK. Increasing irradiation temperature maximizes vitamin E grafting and wear resistance of ultrahigh molecular weight polyethylene. *Journal of Biomedical Materials Research Part B: Applied Biomaterials*. 2013;101B(3):436 – 440.
- [27] Lewis G. Properties of crosslinked ultra-high-molecular-weight polyethylene. *Biomaterials*. 2001;22(4):371 – 401.
- [28] International Organisation for Standardization. *ISO 7500-1 Metallic materials - Verification of static uniaxial testing machines, Part 1: Tension/compression testing machines - Verification and calibration of the force measuring system*; 2004.
- [29] Son S, Lim H, Ahn J. The effect of vibration cutting on minimum cutting thickness. *International Journal of Machine Tools and Manufacture*. 2006;46(15):2066 – 2072.
- [30] Lai X, Li H, Li C, Lin Z, Ni J. Modelling and analysis of micro scale milling considering size effect, micro cutter edge radius and minimum chip thickness. *International Journal of Machine Tools and Manufacture*. 2008;48(1):1 – 14.
- [31] Carr JW, Feger C. Ultraprecision machining of polymers. *Precision Engineering*. 1993;15(4):221 – 237.

## A P values from ANOVA

Table 6: P values for main effects and interactions, from ANOVA. Values less than 0.001 are rounded to 0.

Factor	Fc	Ft	Ra	Chip thickness
Material	0	0.002	0	0
Rake angle	0	0	0	0
Sharpness	0	0	0	N/A
Cutting speed	0.022	0.016	0.093	0.172
Depth of cut	0	0	0	0.021
M*R	0.001	0	0	0.007
M*S	0.005	0.002	0	N/A
M*CS	0.118	0.048	0.001	0.171
M*DOC	0.045	0.182	0.008	0.021
R*S	0	0	0	N/A
R*CS	0.261	0.087	0.025	0.131
R*DOC	0	0	0	0
S*CS	0.002	0.001	0	N/A
S*DOC	0.07	0	0	N/A
CS*DOC	0.548	0.406	0.155	0.468
M*R*S	0.003	0	0	N/A
M*R*CS	0.448	0.185	0.001	0.291
M*R*DOC	0.078	0.125	0.001	0.065
M*S*CS	0.292	0.277	0	N/A
M*S*DOC	0.796	0.705	0.005	N/A
M*CS*DOC	0.68	0.722	0	0.009
R*S*CS	0.471	0.188	0.005	N/A
R*S*DOC	0.024	0.006	0	N/A
R*CS*DOC	0.358	0.079	0.389	0.455
S*CS*DOC	0.339	0.596	0.038	N/A
M*R*S*CS	0.783	0.534	0	N/A
M*R*S*DOC	0.437	0.265	0.001	N/A
M*R*CS*DOC	0.406	0.303	0	N/A
M*S*CS*DOC	0.912	0.884	0	N/A
R*S*CS*DOC	0.022	0.014	0.017	N/A
M*S*R*CS*DOC	N/A	N/A	0	N/A

## B Notation

AOX	UHMWPE with antioxidant additives
DMA	Dynamic Mechanical Analysis
<i>DOC</i>	Depth of cut
DSC	Differential Scanning Calorimetry
FTIR	Fourier Transform Infrared Spectroscopy
GUR 1020	Blend of UHMWPE produced by Ticona
<i>r</i>	Edge radius of cutting tool
SEM	Scanning Electron Microscope
UHMWPE	Ultra High Molecular Weight Polyethylene
UTS	Ultimate Tensile Strength
XLK	UHMWPE which has been crosslinked